Ferromagnetic resonance in metallic multilayers. II. Numerical example and semiquantitative model*

G. Spronken,† A. Friedmann, and A. Yelon
Engineering Physics Department, Ecole Polytechnique, Montreal H3C 3A7, Quebec, Canada
(Received 10 November 1976)

In the preceding paper, we have presented a method for analyzing the ferromagnetic resonance behavior of multilayer films. We present first the results for a relatively simple case. Then, a simple model is presented which yields the major features of the results of the rigorous calculation. With this model, it is possible to predict what will happen in a given situation and to develop an image of the internal magnetizations during resonance.

I. INTRODUCTION

In the preceding paper[1] (hereafter referred to as I), we presented an approximate theoretical solution of the problem of ferromagnetic resonance (FMR) in metallic multilayers under the following restrictions: (a) weak diffusion between the layers; (b) the direction of the dc magnetization near the interface between two layers does not vary to greatly from the direction far from this interface. Even with these restrictions, the numerical applications are limited at present to the particular cases in which it is possible to ignore the antiresonant polarization wave in each phase. In this article we will study, as a simple application of the method, the case of a sample with total symmetry consisting of two similar phases. The anisotropy at the interfaces is assumed to be weak and the spins are pinned at the external surfaces. This structure is shown in Fig. 1.

The external layers have the properties of Ni, and the central layer is a hypothetical material with physical constants close to those of Ni. These are presented in Table I. In this particular case, where we can neglect the nonresonant wave, the problem has six unknowns. Consequently, from the point of view of the numerical treatment, the FMR problem becomes simpler than for a two-layer film with eight unknowns.

In Sec. II, we shall find the static magnetization directions for this structure. In Sec. III, we obtain the dispersion relations, and absorbed power.

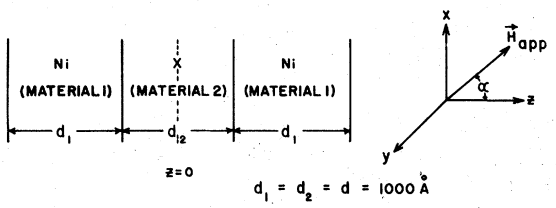

FIG. 1. Multilayer structure.

Then, in Sec. IV, we present a simple interpretation of the behavior of each layer and the effect of the interfacial exchange. Finally, in Sec. V, we shown that the model yields resonance spectra in qualitative agreement with the results of Sec. III.

II. STATIC PROBLEM

Before applying the calculations of I to our case, one must be sure that the directions of the magnetization obey the two conditions presented there: condition (i):

$$|\theta_{ij} - \theta_{0j}| \text{ small}, \quad j = 1, 2;$$

condition (ii):

$$D_j \ll d_j, \quad j = 1, 2.$$

θ_{0j} is the angle of the dc magnetization far from the interface in layer j, θ_{ij} the angle at the interface, D_j the distance from the interface where the angle attains the value θ_{0j}, and d_j the thickness of

TABLE I. Physical constants of the two materials.

	A (erg/cm)	λ (sec^{-1})	γ (Oe^{-1})	σ (sec^{-1})	M_0 (Oe)
Ni	0.81×10^{-6}	0.375×10^{8}	0.193×10^{8}	0.142×10^{17}	484.0
X	0.80×10^{-6}	0.377×10^{8}	0.194×10^{8}	0.143×10^{17}	524.0

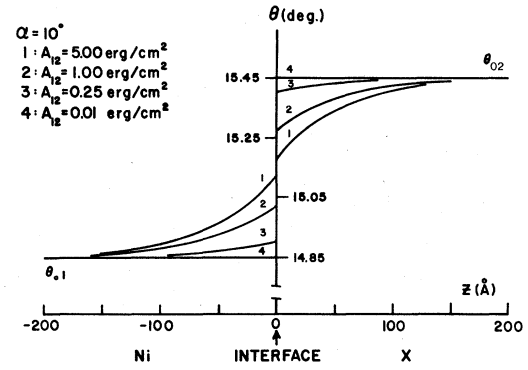

FIG. 2. Magnetization direction near an interface for $\alpha = 10°$, with different values of the coupling constant A_{12}.

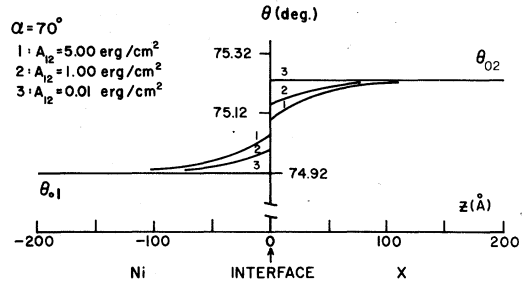

FIG. 4. Magnetization direction near an interface for $\alpha = 70°$, with different values of the coupling constant A_{12}.

the layer. For $\theta = 0°$ and $\theta = 90°$, i.e., when the field $\vec{H}_{app}$ is normal or parallel to the sample surface (Fig. 1) the above conditions are automatically satisfied. In fact, in both cases the dc magnetizations ($\vec{M}_{01}$ and $\vec{M}_{02}$) are parallel to the applied field in the whole sample, including the interfaces.

When $\vec{H}_{app}$ is at an arbitrary angle with respect to the normal to the surface, the directions of the dc magnetizations are different in each layer, and near the interface there is a region in which the magnetization direction varies. For our example, the variations of the directions of the dc magnetizations are given in the Figs. 2–4 for different values of α and of coupling parameter A_{12}. These curves are obtained by solving Eqs. (32) of I. The variation of magnetization in the z direction (which is also the propagation direction for the electromagnetic wave) is monotonic regardless of the magnitude of the coupling parameter A_{12}. For the parameters chosen, the gradients of the angles remain small even for large A_{12}. Both for the internal and external layers, the difference between the angle at the interface θ_{ij} and the angle θ_{0j} far from the interface is smaller than 0.5°, i.e., condition (i) is fulfilled. We also note, from the curves of Figs. 2–4, that D_1 and D_2, where $\theta_1(D_1)$ and $\theta_2(D_2)$ reach the asymptotic values θ_{01} and θ_{02} are small (~100 Å) in comparison with the thicknesses of the layers ($d = 1000$ Å). Thus, condition (ii) is also fulfilled. Consequently, the restrictions concerning the directions of the dc magnetizations are obeyed and we can expect that, at least to a first approximation, the wave vectors have the same values at the interface as in the bulk, and the wave at the interface is identical to that in the volume. The continuity equations [Eqs. (35) and (36) of I] connecting the amplitudes of the waves in the two phases at the interface are sufficient to describe (to first order) the behavior of the resonant polarization waves and can be used to solve the FMR problem for the case to be studied.

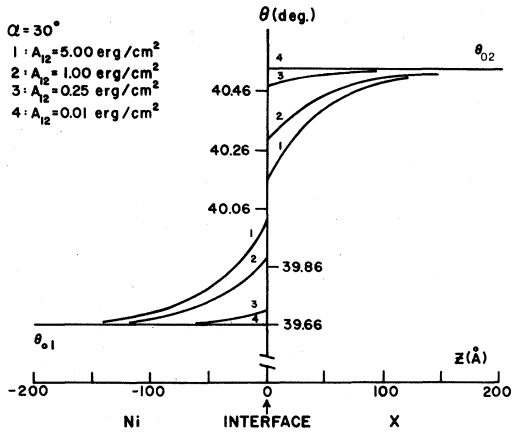

FIG. 3. Magnetization direction near an interface for $\alpha = 30°$, with different values of the coupling constant A_{12}.

III. DYNAMIC PROBLEM: DISPERSION RELATIONS

Experimentally, the study of the FMR is made using a field sweep. However, since a frequency sweep calculation is simpler to perform (as $\vec{H}_{app}$, and hence the magnetization directions, remain constant), we will describe such a calculation here. First, we choose a value of the applied field ($\vec{H}_{app}$) so that for $\alpha = 0$, the ferromagnetic resonance frequency (uniform precession) of the nickel layer is $f = 36$ GHz (Q band):

$$H_{app} = 2\pi f/\gamma_1 + 4\pi M_{01} = 17\,802 \text{ Oe}.$$

The calculation will work as long as H_{app} is large enough to saturate the sample, as it is in this case. From Eqs. (7) of I, one obtains the angles θ_{01} and θ_{02} at equilibrium in each phase for each

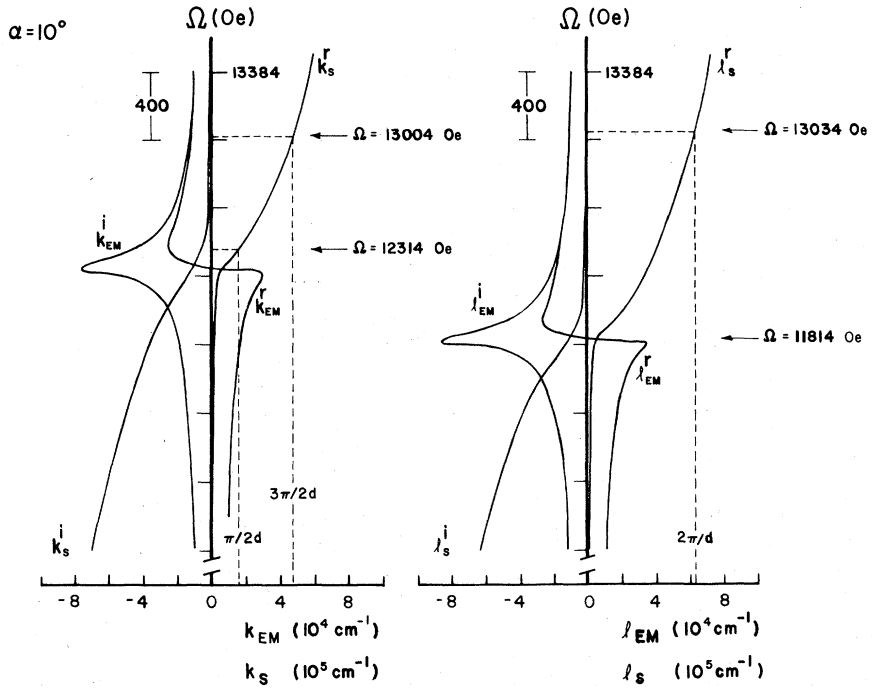

FIG. 5. Dispersion relation for the resonant components in each layer. $\alpha = 10°$. The wave vectors in the outer (Ni) layers are represented by k, those in the inner (X) layer by l.

direction of dc applied magnetic field (α). Then from Eqs. (6) and (7) of I, one obtains the values of the internal fields

$$H_{0j} = -4\pi M_{0j}\cos^2\theta_{0j} + [H_{\text{app}}^2 - (2\pi M_{0j}\sin 2\theta_{0j})^2]^{1/2}, \quad j = 1, 2.$$

From this expression one then obtains the resonance frequencies for uniform precession in each layer. These are given by

$$\Omega_j = \omega_j/\gamma_j = (H_{0j}^2 + 4\pi M_{0j} H_{0j}\sin^2\theta_{0j})^{1/2}, \quad j = 1, 2.$$

We then chose an average frequency

$$\Omega^0 = \tfrac{1}{2}(\Omega_1 + \Omega_2)$$

and sweep the frequency around this value.

For each direction of the applied field it is then

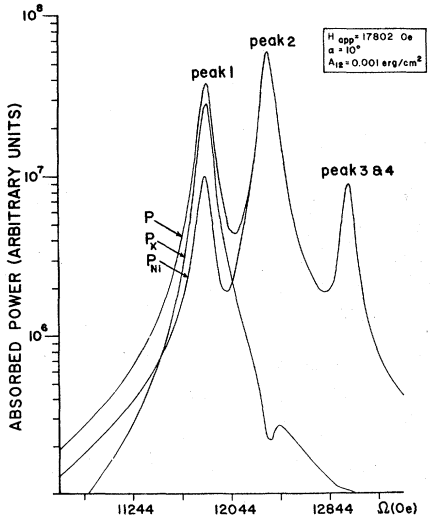

FIG. 6. Absorbed power spectra for $\alpha = 10°$, $A_{12} = 10^{-3}$ erg/cm^2. P represents the power absorbed by the whole sample; P_X is the power absorbed in the inner layer; P_{Ni} is the power absorbed by the outer layers.

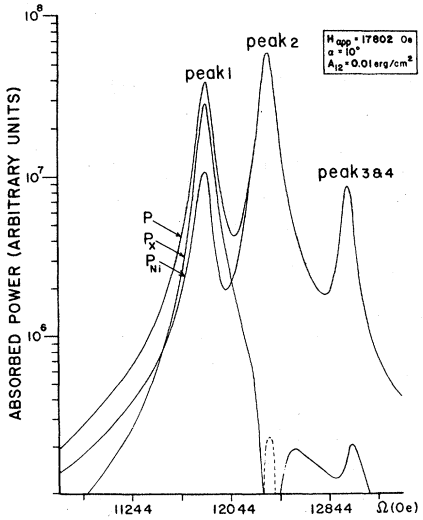

FIG. 7. Absorbed power spectra for $\alpha = 10°$, $A_{12} = 10^{-2}$ erg/cm^2. For the part of P_X indicated by dotted lines, the power absorption is negative.

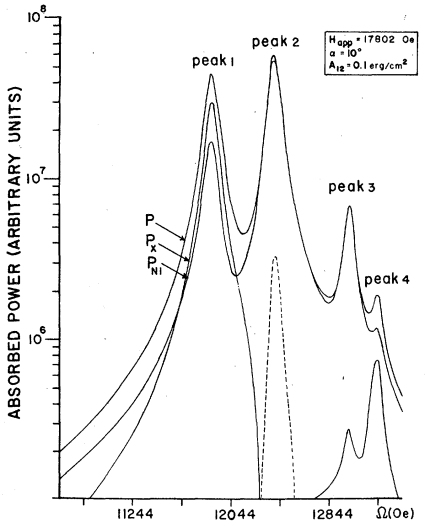

FIG. 8. Absorbed power spectra for $\alpha = 10°$, $A_{12} = 0.1$ erg/cm^2.

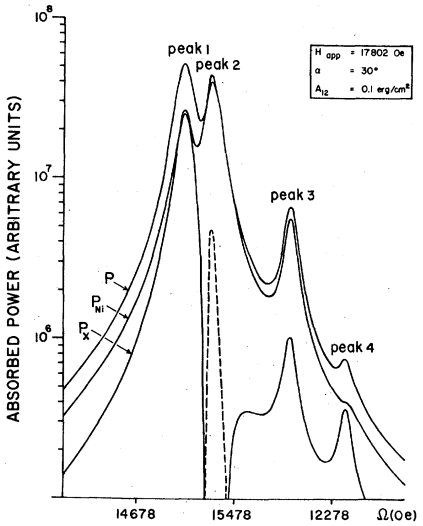

FIG. 10. Absorbed power spectra for $\alpha = 30°$, $A_{12} = 0.1$ erg/cm^2.

possible to obtain the wave vectors from the dispersion relation Eq. (16) of I for all the values of Ω around Ω^0. In Fig. 5, these are given for a given orientation of $\vec{H}_{app}(\alpha = 10°)$. In order to simplify the notation we denote as $\vec{k}_{EM}$ and $\vec{k}_S$ the wave vectors associated with the electromagnetic or uniform precession branch (EM) and the spin-wave branch for the external layer and $\vec{l}_{EM}$ and $\vec{l}_S$ for the internal layer. The real and imaginary parts of these vectors are denoted by a superscript (r or i). Knowing these wave vectors, we can construct the resonant polarization waves in each layer, the rf magnetic fields, and the rf electric fields, as outlined in I. The simultaneous solution of the continuity equations at the interfaces and the external faces then gives the power absorption spectra for the whole system, and for the individual layers. In Figs. 6–12 these spectra are drawn for different directions of the applied field, and for different values of the coupling A_{12} between the layers. In Secs. IV and V we shall show that it is possible to understand the general behavior of these spectra by assuming that the waves in the different layers may be described by simple tri-

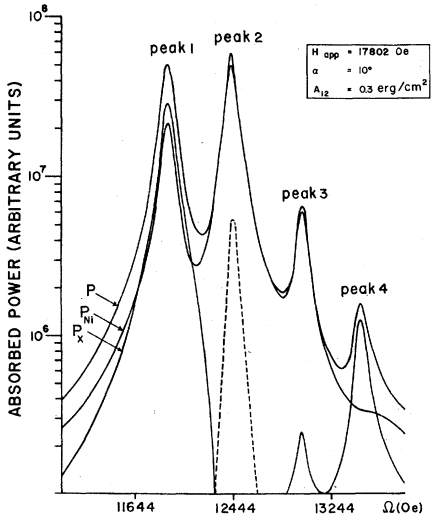

FIG. 9. Absorbed power spectra for $\alpha = 10°$, $A_{12} = 0.3$ erg/cm^2.

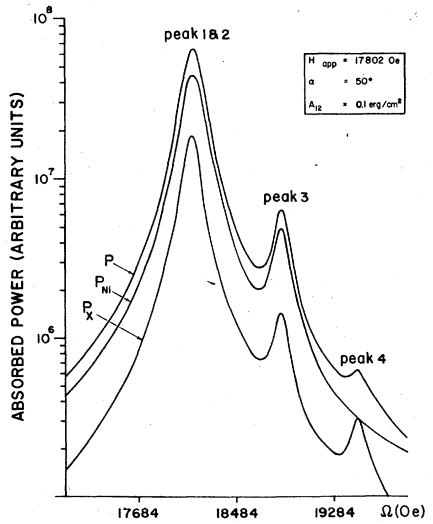

FIG. 11. Absorbed power spectra for $\alpha = 50°$, $A_{12} = 0.1$ erg/cm^2.

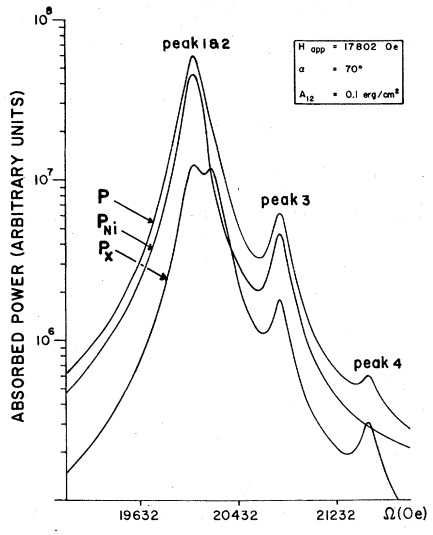

FIG. 12. Absorbed power spectra for $\alpha = 70°$, $A_{12} = 0.1$ erg/cm^2.

gonometric functions. We may then predict the positions of the resonance peaks quite accurately.

IV. EFFECT OF COUPLING ON RESONANT WAVES

Let us now consider the resonant (right-hand precession) excitations in the external layer μ^+ and in the internal layer ξ^+. These may be expressed as

$$\mu^+ = \mu^+_{EM} + \mu^+_S , \tag{1}$$

$$\xi^+ = \xi^+_{EM} + \xi^+_S . \tag{2}$$

In Eqs. (1) and (2), EM indicates the electromagnetic (or uniform precession) excitation and S the spin-wave excitation. The four waves on the right-hand side of Eqs. (1) and (2) are sine and cosine functions with complex arguments. While it is known that both the EM and S waves will be excited in almost any situation, and that they may be excited with nearly equal amplitude in special cases,[2] in general, either one or the other will be dominant. In particular, near the ferromagnetic resonance Ω_j, the EM wave will be strongly excited, while at higher frequencies, spin waves may be strongly excited [spin-wave resonance (SWR)]. For the S wave, the real part will be more important than the imaginary part, as shown in Fig. 5. If this is the case, μ^+ or ξ^+ can be approximately described by a real sine or cosine function. In what follows, we shall assume that this is the case, and shall show that in most cases we obtain good agreement between this simple, frequently used model and the rigorous calculations of I.

A. Zero coupling

Here, and in what follows, we consider the wavelengths allowed by the boundary conditions without asking what will be the intensity of the resonance or whether power will be absorbed at all. In the absence of coupling between the two layers, the continuity equations for the waves μ^+ and ξ^+ at the interface reduce to spin unpinned conditions

$$\left.\frac{\partial \mu^+}{\partial z}\right|_{z=d/2} = 0 , \tag{3}$$

$$\left.\frac{\partial \xi^+}{\partial z}\right|_{z=d/2} = 0 . \tag{4}$$

Since, in our example, the spins are pinned at the external faces, we have, at $z = \frac{3}{2}d$,

$$\mu^+ = 0 . \tag{5}$$

The wave in the inner layer must obey Eq. (4) and the only possible solution, that shown in Fig. 13,

$$l^r = 2\pi n/d, \quad n = 0, 1, 2, \ldots . \tag{6}$$

For $n = 0$, we have uniform precession in the inner layer and $l \approx 0$. For $n \geq 1$, we have SWR. For the outer layer, the wave must fulfill the conditions of Eqs. (3), (5). Thus we have (Fig. 13)

$$k^r = (2m+1)\pi/2d, \quad m = 0, 1, 2, \ldots . \tag{7}$$

There is no uniform precession in the external layer.

Using the dispersion relation of Fig. 5, we find that, for $m = 0$, $\Omega = 12\,314$ Oe; for $m = 1$, $\Omega = 13\,004$ Oe; for $n = 0$, $\Omega = 11\,814$ Oe; and for $n = 1$, $\Omega = 13\,034$ Oe. These correspond fairly closely with peaks 2, 3, 1, and 4, of Fig. 6, which is for very weak coupling.

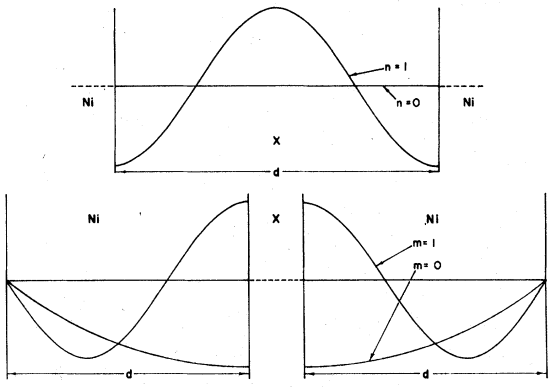

FIG. 13. Approximate wave shapes in the three layers at zero coupling.

B. Arbitrary coupling

In the case of arbitrary coupling, the continuity equations for resonants waves at the interfaces are given in I:

$$\mu^+ - \frac{A_1}{A_{12}} \frac{\partial \mu^+}{\partial z} - \frac{M_{01}}{M_{02}} \xi^+ = 0 , \tag{8}$$

$$\xi^+ + \frac{A_2}{A_{12}} \frac{\partial \xi^+}{\partial z} - \frac{M_{02}}{M_{01}} \mu^+ = 0 . \tag{9}$$

From the pinning conditions given above, μ^+ and ξ^+ must be approximately described at frequencies $\Omega > \Omega_2$ by

$$\mu^+ = C \sin k_S^r (z - \tfrac{3}{2} d) , \tag{10}$$

$$\xi = D \cos l_S^r z . \tag{11}$$

Combining Eqs. (8)–(11), we obtain a pair of homogeneous equations:

$$\begin{pmatrix} -\sin k_S^r d - (A_1/A_{12}) k_S^r \cos k_S^r d & -(M_{01}/M_{02}) \cos l_S^r \tfrac{1}{2} d \\ (M_{02}/M_{01}) \sin k_S^r d & \cos l_S^r \tfrac{1}{2} d - (A_2/A_{12}) l_S^r \sin l_S^r \tfrac{1}{2} d \end{pmatrix} \begin{pmatrix} C \\ D \end{pmatrix} = 0 . \tag{12}$$

This system has a nontrivial solution only if the determinant of the coefficients vanishes. This implies

$$A_{12} = \frac{A_1 A_2}{(A_1/l_S^r) \cot l_S^r \tfrac{1}{2} d - (A_2/k_S^r) \tan k_S^r d} . \tag{13}$$

This characteristic equation gives the relation between allowed values of k_S^r and of l_S^r for arbitrary values of A_{12}.

In the above form, this transcendental equation has the advantage that it can be solved simultaneously with the dispersion relations. For each value of Ω ($\Omega > \Omega_2$) we obtain the quantities k_S^r and l_S^r from the dispersion relations and we can then calculate the right-hand side of Eq. (13). For a given value of the coupling, the position of the resonance peaks is obtained by comparing, for each value of Ω, the right-hand side and A_{12}. The value of Ω for which the two are equal is a resonant frequency. There is a series of resonances for a given value of A_{12}.

In the neighborhood of Ω_2, the EM branches will be strongly excited. In this case, the trigonometric function description will not be appropriate, especially if the S branch is also excited. Therefore in what follows, we shall limit ourselves to the study of the behavior of the peaks that are not in the neighborhood of the uniform precession in the central layer. However, the qualitative behavior will be the same for these peaks as for the others. In order to be more specific, we shall use Eq. (13) to describe the evolution of the peaks 2–4 when the direction of the fields $\vec{H}_{app}$ is at angles of $\alpha = 10°$ and $\alpha = 30°$, and that of peaks 3 and 4 at $\alpha = 50°$. In the latter case, peak No. 2 is close to peak No. 1, corresponding to the uniform precession in the inner layer, and its behavior can no longer be described by Eq. (13).

V. ABSORBED POWER SPECTRA

In Figs. 6–12, we have plotted the spectra of power P absorbed by the whole sample, for the first two orders (n or $m = 0, 1$) for each layer, for various coupling constants and for various orientations of the static magnetic field. In Figs. 14–16, we show the resonant peak positions as a function of coupling for 10°, 30°, and 50°. The solid lines represent the results of Eq. (13). For all angles, the agreement between these values and those obtained from Figs. 6–12 is within a few Oe. For arbitrary coupling, the agreement is always better than 20 Oe. The dotted lines show results from Figs. 6–12 for the cases in which Eq. (13) is not applicable.

Generally, the peaks shift towards higher frequency as the coupling increases, eventually reaching the asymptote given by the continuity equation

$$M_{02} \mu^+ = M_{01} \xi^+ , \tag{14}$$

which is the limiting result of Eqs. (8) and (9) for

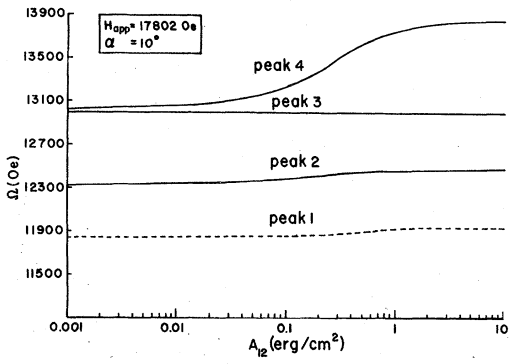

FIG. 14. Resonant peak positions as a function of coupling strength for $\alpha = 10°$.

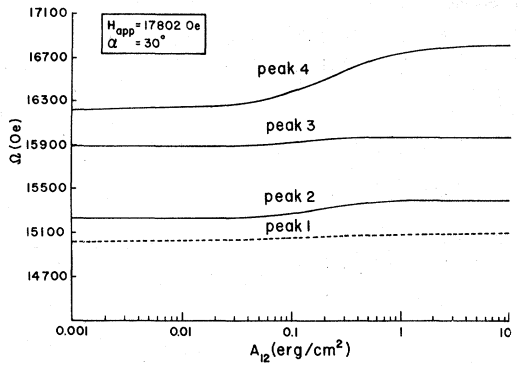

FIG. 15. Resonant peak positions as a function of coupling strength for $\alpha = 30°$.

A_{12} infinite. There are, however, exceptions to this rule, such as peak No. 3 for $\alpha = 10°$ and peak No. 2 for $\alpha = 50°$.

Figures 17–20 show the waves in the different media (determined by the methods of I) for the four peaks discussed above for 10°. The layer which is in resonance induces an excitation in the other layer, which tends to increase with increasing coupling, as the two layers approach being in phase at the interface. This brings about a decrease of the wavelength as compared with the uncoupled situation (Fig. 5) and thus an increase in the resonant frequency.

It is clear from Fig. 19 why peak No. 3 does not move. In this part of the spectrum, there is about $\frac{3}{4}$ of a wavelength in the external layer and one wavelength in the central layer. Therefore the wave derivatives are very small at the interface and the continuity equations are satisfied, whatever the value of the coupling, by waves which are in phase. The same phenomenon takes place in the case of peaks 1 and 2 for $\alpha = 50°$ (Fig. 16). The first SWR takes place in the external layer near

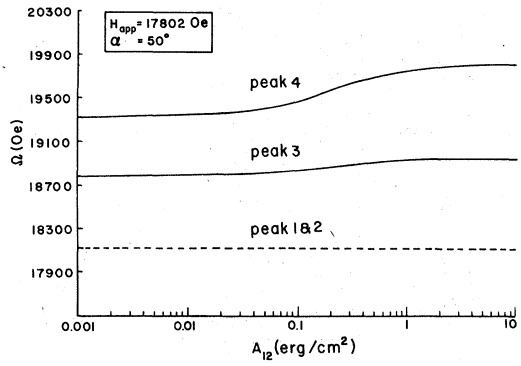

FIG. 16. Resonant peak positions as a function of coupling strength for $\alpha = 50°$.

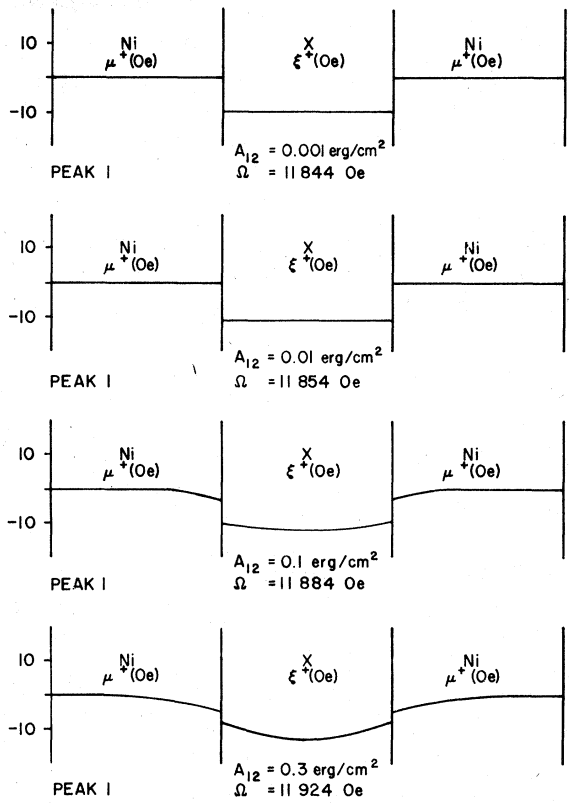

FIG. 17. Wave shapes at resonance, peak No. 1, at different coupling strengths. $\alpha = 10°$.

the same frequency as the uniform precession in the inner layer. We then have almost a quarter wavelength in the nickel layer and one wavelength in the inner layer. The wave derivatives are therefore weak at the interface and the position of the peak and the coupling has very little bearing on the position of the peak. This kind of phenomenon can obviously occur quite often.

Let us now extend our discussion slightly, to consider which waves described above, can actually absorb power. It is clear that at zero coupling the $n = 1$ wave (Fig. 13) which is responsible for peak No. 4 absorbs negligible power, as is usually the case for single films with unpinned surfaces (in which only the uniform precession will absorb strongly). For strong coupling, this peak shifts to higher frequencies, the wave vectors increase, and the absorbed power becomes appreciable.

The negative value of P_x for peak No. 2 at strong coupling corresponds to the fact that the external layers drive the internal layer more than 90° out of phase with the applied rf field. One would calculate the same thing if one concentrated on small regions of a single film undergoing SWR.

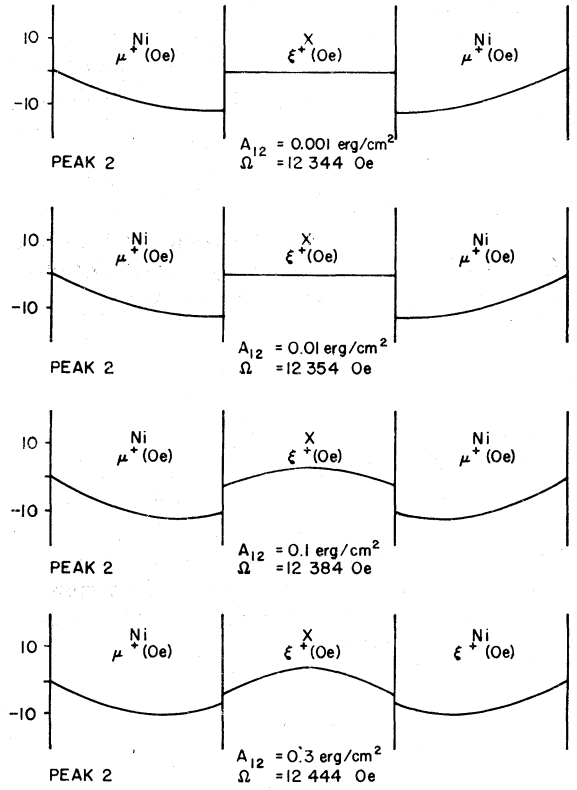

FIG. 18. Wave shapes at resonance, peak No. 2, at different coupling strengths. $\alpha = 10°$.

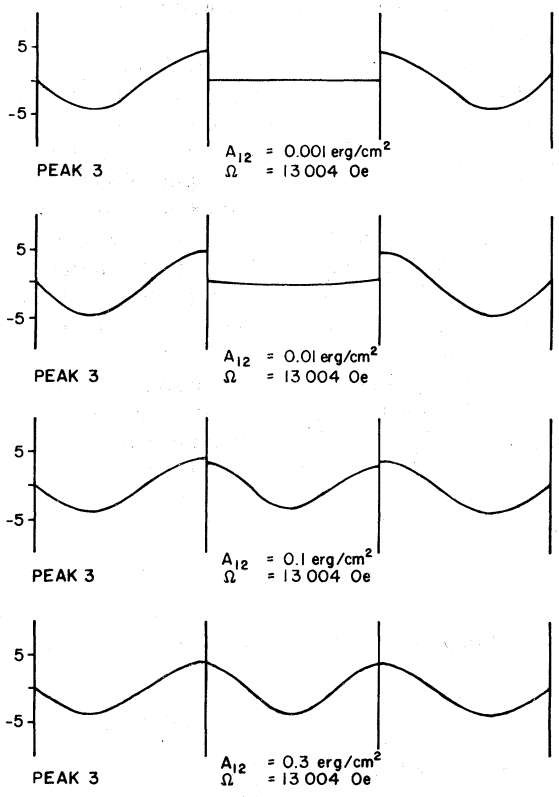

FIG. 19. Wave shapes at resonance, peak No. 3, at different coupling strengths. $\alpha = 10°$.

VI. DISCUSSION

Through this particular example, we have shown that it is possible to understand and interpret the gross feature absorbed power spectra of multilayer films starting from a simple model. This model is no longer valid in the uniform precession regions of one of the layers. We have shown, however, that the physical behavior of the sample (evolution of the spectra, modifications in the shapes of the waves in the two layers when the coupling varies) is the same for the whole spectrum, regardless of the type of resonance, SWR, or uniform precession. Consequently, the value of the coupling between the layers can be determined experimentally starting from any resonance peak. We choose one of the peaks, and proceed as follows: We obtain position Ω of one of the resonance peaks from experimental results, and then, by solving the dispersion relations for this frequency, we obtain wave vectors $\vec{k}_S$ and $\vec{l}_S$. From these we can determine the coupling.

As Hoffmann has pointed out,[3] the multilayer approach can have advantages over the study of single films for the understanding of surface and interface effects in resonance. We might point out that it is possible to include the effects of interfacial anisotropy, which we have neglected in this paper, without great difficulty. In fact, the same method which has been presented in I can be applied to the study of single films with surface anisotropy, as long as the magnetization near the surface obeys the conditions presented in I and

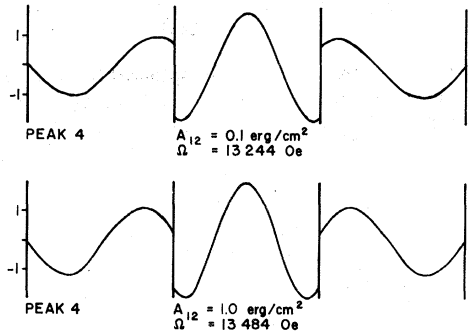

FIG. 20. Wave shapes at resonance, peak No. 4, at different coupling strengths. $\alpha = 10°$.

emphasized in Sec. II of this paper. We are presently engaged in such an investigation.[4]

In the more complicated cases, in which we must take into account the waves of both resonant and nonresonant polarization in each layer, it has not yet been possible to solve the problem due to difficulties in the numerical treatment.[1] We believe, however, that even in these cases, the method used here to explain the results of our example remains valid, at least qualitatively. This hypothesis is based on the fact that the nonresonant waves are always weakly excited.[1]

---

*Supported in part by the National Research Council of Canada.

†Present address: Groupe des Transitions de Phases, C.N.R.S., 38042 Grenoble Cedex, France.

[1]G. Spronken, A. Friedmann, and A. Yelon, preceding paper, Phys. Rev. B 15, 5141 (1977).

[2]Y. J. Liu, R. C. Barker, and A. Yelon, AIP Conf. Proc. 18, 1285 (1973); *Proceedings of the International Conference on Magnetism ICM 73* Nauka, Moscow, 1974), Vol. IV, p. 534.

[3]F. Hoffmann, Doctoral thesis (Université de Paris-Sud, 1971) (unpublished).

[4]H. T. Quach, A. Friedmann, C. Y. Wu, and A. Yelon, Proceedings of the Eighth International Colloquium on Thin Films, University of York, 1976, p. 99 (unpublished).